Surveillance Radar Range-Bearing Centroid Processing

Benjamin J. Slocumb

Georgia Tech Research Institute, Georgia Institute of Technology, Atlanta, GA 30332-0840, USA

ABSTRACT

In non-monopulse mechanically scanned surveillance radars, each target can be detected multiple times as the beam is scanned across the target. To prevent redundant reports of the object, a centroid processing algorithm is used to associate and cluster the multiple detections, called primitives, into a single object measurement. This paper reviews several techniques for centroid processing, and presents a new center of mass algorithm that is implemented with the recursive least squares algorithm. The new algorithm has a unique gating process to enable the primitive measurement association. Simulation results of the new algorithm are reported. Multiple object merged measurement handling issues within the centroid processing context are discussed.

Keywords: Surveillance Radar, Range-Bearing Estimation, Centroid Processing, Target Tracking

1. INTRODUCTION

Surveillance radars typically are long-range two-dimensional (range and bearing) mechanically scanned sensors used to provide early warning against airborne platforms. Monopulse (dual-feed) processing is widely used in modern tracking radars where precise angle measurements are critical. However, the cost for a monopulse antenna and receiver is substantially higher. Many surveillance radars are non-monopulse for cost or installation reasons, and target azimuth estimation must be achieved through a *centroid processing* scheme.

A wide azimuth antenna beam is common in surveillance radars because a low RF frequency is employed (for better propagation properties) and the dimension of the antenna may be limited by installation concerns. Further, a wide beamwidth can be desired because (i) it allows the target to be detected multiple times thereby improving the overall target detection likelihood, and (ii) multiple measurements may be required to perform range-resolve processing when certain Doppler waveforms are employed.

When a wide azimuth beamwidth is used, each target is detected multiple times in adjacent range-bearing cells. For this paper, we will define these detections to be *primitives*[1] with associated parameters $\{R(n), B(k), A(n,k)\}$. Here, $R(n)$ is the range of the nth range bin, $B(k)$ is the bearing of the kth azimuth cell, and $A(n,k)$ is the voltage sample of the target amplitude at the output of the envelope detector for range-azimuth cell (n,k). Figure 1 shows a range-bearing map where multiple primitives of the same object are collect over a single scan.

The fundamental problem addressed in this paper is the signal processing requirement to combine multiple adjacent primitives into a single object measurement report. Without this processing, ambiguities occur in tracking occur because redundant measurements (the collection of primitives) of the same object would be reported. An estimation procedure is used to *associate and cluster* the primitives, and to refine the target range-bearing estimate. The logic associated with the centroid processing technique must allow for missed detections, support conditions where the target has a large extent, and handle the case of multiple closely spaced targets. Further, the logic to combine adjacent primitives must be matched to the radar beamwidth and scan rate and be integrated with any range-resolve processing.

This paper is organized as follows. Section 2 discusses aspects of the surveillance radar system model that influence the centroid processing algorithm. Section 3 presents a review of centroid processing techniques discussed in the literature. Section 4 describes a new centroid processing algorithm that is based on the recursive least squares algorithm. Section 5 presents some simulation results, and Section 6 provides conclusions from the study.

Other author information: Send correspondence to Email: ben.slocumb@gtri.gatech.edu; Telephone: 404-894-8239; Fax: 404-894-8636.

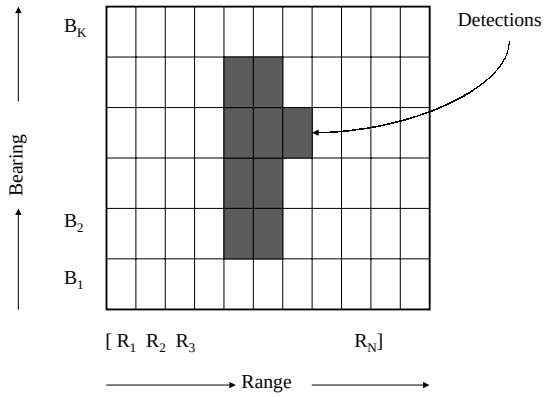

Figure 1. Diagram showing the detection data in a range-bearing grid.

2. SURVEILLANCE RADAR MODEL

2.1. General requirements on surveillance radars

The general requirements for a military surveillance radar are to provide a good long-range target detection capability with a modest ability to locate targets (in range and bearing) for acquisition/tracking radar cuing. In modern applications, a target tracking capability in the surveillance radar is desired to maintain good situation awareness over the air picture. The requirement to survey a large air space competes with the desire to provide high-quality measurements to support a tracker at a modest update rate. Meanwhile, the desire to use Doppler processing to handle clutter competes with the desire to have a long unambiguous target detection range.

An important radar system parameter that determines the centroid processing accuracy is the number of detections (i.e., pulses) available when the radar antenna scans across the object. From Skolnik[2] pg. 2.16 the number of pulses received between the half-power beamwidth is computed as

$$N_{AZ} = \frac{\Theta_{AZ\_deg}}{6 \cdot \mathrm{PRI} \cdot \mathrm{RPM} \cdot \cos(e_i - \hat{e})} \tag{1}$$

where Θ_{AZ_deg} is the half-power azimuth beamwidth measured in degrees, PRI is the pulse repetition interval, RPM is the rotation rate of the antenna, e_i is the ith target elevation, and $\hat{e}$ is the elevation pointing angle of the mechanical antenna. The $\cos(e_i - \hat{e})$ accounts for the apparent azimuth beamwidth change with respect to the target elevation. The maximum unambiguous range is given by $R_u = c \cdot \mathrm{PRI}/2$. If we make the substitution for $\mathrm{PRI} = 2R_u/c$, then

$$N_{AZ} = \frac{\Theta_{AZ\_deg} \cdot c}{6 \cdot R_u \cdot \mathrm{RPM} \cdot \cos(e_i - \hat{e})} \tag{2}$$

This expression shows that to maximize N_{AZ}, which is desired to enhance the azimuth estimation accuracy, then there are two choices: one is to slow the rotation rate of the antenna, the other is to reduce the unambiguous range of the radar. Reducing the rotation rate has the negative impact that the surveillance update rate of the air picture is reduced. The reduced unambiguous range is undesirable unless the radar is able to conduct range resolve processing by using alternate PRI values within the beam time-on-target.

If the radar is using coherent processing for clutter suppression (discussed in Section 2.2), then PRI switching is possible after each coherent dwell. If the number of pulses in a Doppler dwell is $N_D = T_D/\mathrm{PRI}$ where T_D is the coherent dwell time, then the number of coherent processing intervals that fit into the time the beam is on the target is $N_{CPI} = N_{AZ}/N_D$. Substituting into (1),

$$N_{CPI} = \frac{\Theta_{AZ\_deg}}{6 \cdot N_D \cdot \mathrm{PRI} \cdot \mathrm{RPM} \cdot \cos(e_i - \hat{e})} \tag{3}$$

To maximize the unambiguous detection range when using multiple PRI range resolve processing (discussed in Section 2.3), there is a mutual requirement to maximize the PRI and the number of CPIs used for processing. Equation (3) shows that to maximize N_{CPI} while holding the PRI constant, then one would have to reduce either N_D or the antenna rotation rate. Reduction of the latter has negative consequences as already discussed, while reduction of the N_D is undesirable since it impacts the Doppler channelization capability and hence the clutter suppression characteristics.

2.2. Doppler processing in low PRF surveillance radar

Traditionally, Doppler processing was avoided in long-range surveillance radars because of the requirement to support a long unambiguous range. However, because Doppler processing is an excellent means for suppressing clutter, a technique[1] used more recently is to employ a low PRF pulse Doppler waveform and to ignore the Doppler ambiguity. The outputs of the Doppler filter bank are merged into two reduced outputs: a moving target output, and a stationary target output. The actual range rate is never estimated. This technique has the advantage that stationary clutter is contained only in the merged stationary Doppler channel output. Typically, two separate CFAR processes are implemented, one for the moving target channel and one for the stationary target channel.

2.3. Range resolve processing

With the use of Doppler processing, the radar is only able to change the PRI after each CPI. Following Morris[3] pg. 202, define the following integers

$$N_i = \lfloor \frac{\text{PRI}_i}{\text{PW}} \rfloor, \quad i \in \{1, \ldots, M\} \tag{4}$$

where PRI_i is the ith PRI in the set and M is the total number in the set. Then the maximum unambiguous range that can be resolved is given by

$$R_u = \text{lcm}(N_1, \ldots, N_M) \cdot \frac{c \cdot \text{PW}}{2} \tag{5}$$

To maximize the number of PRIs available for range resolve processing, one would set $M \equiv N_{CPI}$. That is, the number of separate PRIs that can be used is governed by the number of CPIs that will fit into the time-on-target of the scanning beam.

Since N_{CPI} determines the number of independent measurements of the target that is received, it is tightly coupled to the achievable azimuth accuracy that can be achieved in a low PRF pulse Doppler surveillance radar using multi-PRI range resolve processing. Given this, one can see that the achievable azimuth accuracy depends on on a number of system parameters including $\{\Theta_{AZ}, N_D, \text{PRI}, \text{RPM}, R_u\}$.

2.4. Cramer-Rao bound on range and bearing

As summarized by Blair,[4] the Cramer-Rao bound for a conventional non-pulse compression radar is approximately

$$\text{var}(\hat{R}) \geq \frac{c^2 \text{PW}}{8 \cdot \text{SNR} \cdot \beta_{IF}} \tag{6}$$

where β_{IF} is the IF bandwidth of the radar. Typically, $\beta_{IF} = 1/\text{PW}$.

The *approximate* Cramer-Rao bound on the azimuth accuracy of a surveillance radar was derived by Swerling.[5] In the derivation, the radar model was specifically for a conventional pulsed radar with no Doppler processing employed. The data model for the problem was given by $\{A(k), B(k); k = 1, \ldots, N\}$ where $A(k) = A(n, k)$ for some n is the target amplitude measured on the output of the radar pulse envelope detector, and $B(k)$ is the measured bearing of the kth pulse. The total number of pulses $N \equiv N_{AZ}$ is determined by the radar beamwidth.

The approximate bound derived by Swerling is

$$\text{var}(\hat{B}) \geq \frac{(0.49)^2 \cdot \Theta_{AZ}^2}{N_{AZ} \cdot \text{SNR}} \tag{7}$$

where it is assumed that $\text{SNR} \gg 1$. See Barton[6] pg. 53 for the translation of the Gaussian beam parameters in Swerling's original work to the formula in (7). To get to this closed-form approximation, Swerling had to make a number of assumptions:

A1. The beam shape is Gaussian.

A2. The bearing resolution ΔB is large enough for statistical independence of the noise received on each pulse return.

A3. The bearing resolution $\Delta B = b(k+1) - b(k)$ is sufficiently small such that (i) the time between pulse transmit and receive yields a small motion of the beam, and (ii) the "averaging process" in the likelihood function can be neglected.

A4. The bearing resolution ΔB is small compared to the beamwidth.

A5. The bearing resolution ΔB is small enough to allow for a certain mathematical approximation (sum replaced by an integral).

The question of interest is: can the the bound on the azimuth accuracy of a coherent radar be approximated in (7) by replacing N_{AZ} with N_{CPI}? This issue is pertinent because the coherent radar only receives target detections after each coherent dwell and not on a pulse-to-pulse basis. Of the assumptions, A3–A5 could be questionable in the coherent radar case. Hence, the bound may not be useful for predicting the accuracy of this type of radar.

2.5. Radar received power

At time $t(k)$, the radar points the beam at bearing-elevation angles $(\hat{b}(k), \hat{e}(k)$. Suppose there are N_T targets, and denote $(b_i(k), e_i(k))t$ to be the bearing and elevation at $t(k)$ of the ith target. Next denote $R(n) = n \cdot \Delta R$ (where $\Delta R = c \cdot \mathrm{PW}/2$) as the range of the leading edge of the nth range bin and $\mathcal{I}_n \subseteq \{1, \ldots, N_T\}$ to be the set of target indices for targets that fall into the nth range bin, i.e., targets with range $R \in [R(n), R(n+1)]$. Then the total power received at time $t(k)$ in the nth range bin is

$$P_r(n,k) = \sum_{i \in \mathcal{I}_n} \frac{\delta_i(n) P_t G^2\left(b_i(k), e_i(k)\right) G_{stc}\left(n\right) G_c \lambda^2 \sigma_i}{(4\pi)^3 L R_i^4} \tag{8}$$

where $\delta_i(n)$ is the bin split fraction for target i in range bin n, P_t is the radar transmit power, $G(b_i(k), e_i(k))$ is the antenna gain towards the ith target, $G_{stc}(n)$ is the sensitivity time control gain for the nth bin, G_c is the pulse compression gain, λ is the wavelength, σ_i is the ith target radar cross section, L is the radar receiver loss, and R_i is the ith target range. Note that since the antenna has a fixed scan time interval, k also references a specific pointing direction $\hat{b}(k)$.

Bin splitting is the event where the returned radar pulse straddles two range bins, thereby dividing the total returned power into the two range bins. Bin splitting occurs because there is always a mismatch between the radar receiver discrete range bin positions and the target range. The fraction of return power from the ith target that falls in the nth range bin is

$$\delta_i(n) = \begin{cases} \mathrm{rem}(R_i/R(n-1))/\Delta R, & R_i \in [R(n-1), R(n)] \\ 1 - \mathrm{rem}(R_i/R(n))/\Delta R, & R_i \in [R(n), R(n+1)] \\ 0, & \text{otherwise} \end{cases} \tag{9}$$

where $\mathrm{rem}(\cdot)$ is the remainder function. As discussed in Section 4, the presence of target bin straddle enables the range estimate to be computed using the power weighted average of the bin range values.

2.6. Antenna pattern

A typical mechanically scanned surveillance radar antenna is a parabolic reflector. The antenna is usually constructed with pattern shaping to control the sidelobe levels. For example, cosine shaping may be used for the azimuth pattern and $\csc^2$ shaping may be used in elevation pattern to give it a constant elevation gain. Given the antenna is pointing at bearing-elevation angles $(\hat{b}, \hat{e})$, then the antenna gain[7] at bearing-elevation angle (b, e) is

$$G_0(b,e) = \frac{4\pi \rho_a a_1 a_2}{\lambda^2} \left| E(b - \hat{b}, a_1, \lambda) \cdot E(e - \hat{e}, a_2, \lambda) \right|^2 \tag{10}$$

where (a_1, a_2) are the dimensions of the antenna and ρ_a is the efficiency. For the cosine antenna pattern,

$$E(\theta, a, \lambda) = \frac{\pi}{4} \left[\mathrm{sinc}\left(\frac{a \sin(\theta)}{\lambda} + \frac{1}{2} \right) + \mathrm{sinc}\left(\frac{a \sin(\theta)}{\lambda} - \frac{1}{2} \right) \right] \tag{11}$$

where $\mathrm{sinc}(x) = \sin(\pi x)/x$. The elevation beam pattern is modified with $\csc^2$ shaping so that the actual gain[7] is

$$G(b,e) = \begin{cases} G_0(b,e) \cdot \frac{\csc^2(e-\hat{e})}{\csc^2(e_1)}, & e_1 < e - \hat{e} < e_2 \\ G_0(b,e), & \text{otherwise} \end{cases} \tag{12}$$

where e_1 and e_2 are the angular limits when $\csc^2$ shaping applies.

In Swerling's derivation of the CRLB, and in other azimuth estimation techniques discussed in Section 3, a Gaussian beam pattern is assumed. The Gaussian model can be made a close approximation to patterns like (12) that are typical in surveillance radars.

3. SURVEY OF METHODS FOR CENTROID PROCESSING

3.1. Overview

In this section we review a number of centroid processing techniques that appear in the literature. In most cases, the techniques are formulated for surveillance radars where the primitives $\{R(n), B(k), A(n,k)\}$ are measured for each pulse transmitted and N_{AZ} measurements are presumed made. The applicability of these techniques to the coherent radar case, where only N_{CPI} measurements are made instead, will be discussed in the next section. Further, most of the references do not discuss aspects of performing refined range estimation within the centroid processing context (i.e., only azimuth estimation is performed).

3.2. Moving window estimator (a.k.a. beamsplit estimator)

This estimator, as discussed by Walker[8] et al., is a simple process that maintains a running count of the pulses (in a given range bin) that exceed a threshold. The window size for the running count is equal to N_{AZ}. Two hit density levels are established, which indicate the beginning and end of the target. If the levels are achieved at bearings $B(k_1)$ and $B(k_2)$, then the target azimuth is estimated as

$$\hat{B}(k) = \frac{B(k_1) + B(k_2)}{2} \tag{13}$$

Since the estimator utilizes a moving window of pulse detections to estimate the target azimuth, it is known as the Moving Window estimator. Also, it is termed a Beamsplit Estimator since the estimate is formed by "splitting" the detections within the beam. Walker[8] et al. call the estimator an End Condition method, and also identify a Scan Density method. The difference between the two is that the latter uses a shorter window of pulse detections when forming (13).

Galati and Struder[9] summarized a number of the problems with the Moving Window estimator. The accuracy is dependent on the SNR, N_{AZ}, and the beam shape. Further, the estimator produces a biased estimate, where the bias is a function of the SNR. Also, the azimuth error does not significantly decrease with increasing SNR because, as the SNR increases, the begin/end points shift away from the center of the beam and the measurements that determine the azimuth estimate remain near the detection threshold.

3.3. Two-pole filter detector/azimuth estimator

Cantrell and Trunk[10] proposed an IIR filter (two pole integrator) for mutual target detection and azimuth estimation. They noted that a difficulty with the Moving Window approach is the requirement to save a large number of pulse returns. Also, a double-loop feedback integrator method by Cooper and Griffiths[11] was biased as a function of SNR and produced poor results (relative to the CRLB). The two-pole integrator differs from the double-loop integrator in that the two poles are *not* required to be in the same location.

The general form of the two-pole filter output is

$$y(n,\ell) = \sum_{k=0}^{\infty} h(k) A(n, \ell - k) \tag{14}$$

where the filter $h(k)$ has the transfer function

$$H(z) = \frac{z^{-1}}{1 + p_1 z^{-1} + p_2 z^{-2}} \tag{15}$$

The values of the poles (p_1, p_2) are found by a search technique, and the optimal values are a function of the number of pulses N_{AZ}. Detection performance for this filter was shown to be within 0.15 dB of the optimum.

The azimuth estimate is formed by processing $y(n, \ell)$. Two azimuth estimators were considered for the two-pole filter: a threshold-crossing beamsplit estimator and a maximum output estimator. The former involves finding the angle $B(k_1)$ for the First Target Detection and the angle $B(k_2)$ for the Last Target Detection. The azimuth is then estimated the same as in (13). The second estimator simply involves detecting the maximum amplitude $y(n, k^\star) = \max_k y(n, k)$ on the output of the two-pole filter. Then $\hat{B}(k)$ is set equal to $B(k^\star)$. The authors found that the threshold-crossing beamsplit procedure had a bias that was a function of the SNR, while the maximum value estimator had a fixed bias value. Hence, they recommended the maximum value estimator. The RMS accuracy of the estimator was reported to be only 15% greater than the CRLB.

3.4. Maximum likelihood azimuth estimator

Swerling[5] showed that the maximum likelihood estimator (MLE) for the bearing was of the form

$$\hat{B} \leftarrow \arg\max_{B_T} \sum_{k=1}^{N} \sqrt{A(k)^2 \cdot g\left(\frac{B_T - B(k)}{c_0 \Theta_{AZ}}\right)} \tag{16}$$

where g is the Gaussian two-way power gain pattern of the antenna, and c_0 is a scalar that converts Θ_{AZ} into a Gaussian beam variance parameter. Note that $A(k)^2$ is proportional to SNR_k.

Bernstein[12] derived the MLE and focused on the case of quantized data, where the target amplitude return was limited such that $A(k) \in \{0, 1\}$. The maximum likelihood estimate $\hat{B}$ was shown to be the estimate that solved the condition

$$\sum_{k=1}^{N_{AZ}} A(k) \cdot w\left(\hat{B} - B(k)\right) = 0 \tag{17}$$

The weight w is a function of the the beam shape, the quantization threshold, and the SNR when the beam is pointed directly at the target (i.e., peak SNR). This estimator is implemented by convolving the pulse amplitude sequence $\{A(k)\}$ with a beam pattern function that is based on possible target estimate $\hat{B}(\ell)$,

$$y(\ell) = \sum_{k=1}^{N_{AZ}} A(k) \cdot w\left(\hat{B}(\ell) - B(k)\right) \tag{18}$$

A zero-crossings analysis is then performed to find to find the value $y(\ell^\star) = 0$, and then $\hat{B} = B(\ell^\star)$.

Galati and Struder[9] developed a "binary Bernstein estimator," where the weights w were quantized into binary values $\{-1, 0, 1\}$. The motivation for this algorithm was that it was easy to implement with a tapped delay line, and the optimal weight values of the Bernstein estimator required knowledge of the peak SNR of the target. The binary implementation requires only specification of two parameters that define the number of zero-weights and the number of ± 1 weights. Analysis showed that the performance of the binary estimator was only $0.5 - 1.0\%$ worse than the non-binary weight estimator. One artifact is that the estimation performance actually gets worse with increasing SNR beyond an algorithm-controlled inflection point.

In newer work, Galati and Struder[13] formulated a maximum likelihood estimator that takes into account missing detections. The MLE expression for this problem takes the form of

$$\left[\sum_{k=1}^{N_{AZ}} A(k) \cdot x(k) \cdot w_1\left(\hat{B}(\ell) - B(k)\right)\right] \cdot \left[\sum_{k=1}^{N_{AZ}} A(k) \cdot x(k) \cdot w_2\left(\hat{B}(\ell) - B(k)\right)\right] = \tag{19}$$

$$\left[\sum_{k=1}^{N_{AZ}} A(k) \cdot x(k) \cdot w_3\left(\hat{B}(\ell) - B(k)\right)\right] \cdot \left[\sum_{k=1}^{N_{AZ}} A(k) \cdot x(k) \cdot w_4\left(\hat{B}(\ell) - B(k)\right)\right] \tag{20}$$

where w_i is one of four weights that are based on the Gaussian two-way power gain pattern and its derivative. A detection event $x(k) \in \{0, 1\}$ modifies the weight. Here, $A(k)$ is considered in its full (not binary) form. Also considered was the use of interpolation to find the best estimate of the zero crossing, and the impact of truncating the weights w_i to a shorter filter length.

3.5. Beam shape centroid estimator

Cole[1] et al. have developed a collection of Association and Clustering algorithms for use in a modern airport surveillance radar. This particular radar uses coherent processing, hence some of the issues discussed in Section 2 were addressed. In this implementation, a different algorithm is selected based on the quality/type of measurements received. Some aspects of the algorithms are tailored to specific properties of their surveillance radar. The following algorithms are employed:

- *Single CPI Measurement.* When only a single primitive is received, then the azimuth of the target is set to $\hat{B}(k) = B(k)$.
- *Beamsplit.* In cases where the measured data are affected by exception conditions (e.g., receiver saturation), a beamsplit estimate of the azimuth is computed, include

$$\hat{B}(k) = \frac{B(k_1) + B(k_2)}{2} \tag{21}$$

  where $B(k_1)$ is the bearing of the first report of the cluster and $B(k_2)$ is the bearing of the last report.
- *Center of Mass.* When primitives are received on adjacent angle cells, but only for one of two CPIs used on each range-angle cell, then the azimuth estimate is formed as

$$\hat{B}(k) = \frac{B(k) \cdot A(k) + B(k+1) \cdot A(k+1)}{A(k) + A(k+1)} \tag{22}$$

- *Interpolation.* When primitives are received on adjacent azimuths and with the same PRIs, then the azimuth estimate is

$$\hat{B}(k) = \frac{B(k) + B(k+1)}{2} + K\left(\log A(k) + \log A(k+1)\right) \tag{23}$$

  where K approximates the slope of the antenna pattern log difference curve.
- *Beamshape Match Processing.* When primitives are received three or more consecutive CPIs on the same PRI, then a beamshape matching algorithm is used. The first step in the algorithm is to compute an error metric to determine if more than one target is present. If $B(k)$ corresponds to the bearing with the largest $A(k)$ in the cluster, then the computed error is

$$\epsilon(k) = \hat{a}(k) \cdot \left[\left(\frac{A(k-1)}{A(k)} - \frac{\hat{a}(k-1)}{\hat{a}(k)} \right)^2 + \left(\frac{A(k+1)}{A(k)} - \frac{\hat{a}(k+1)}{\hat{a}(k)} \right)^2 \right] \tag{24}$$

  where $\hat{a}(k)$ is the *predicted* amplitude based on the known antenna pattern. The error calculation is actually "iterated" using a number of finer-spaced beam positions, and the minimum retained. The value of $\epsilon(k)$ is compared to a threshold η. If $\epsilon(k) < \eta$, then a single target is reported with azimuth estimate corresponding to position of the finer-spaced beam that produced the minimum $\epsilon(k)$. If $\epsilon(k) > \eta$, then two targets are reported. The azimuth estimate of the two targets is generated using a "modified beam splitting algorithm" that is not described.

4. NEW RECURSIVE LEAST-SQUARES CENTROID PROCESSING ALGORITHM

4.1. Algorithm for range-bearing centroid processing

This section describes a new algorithm that expands upon previously developed concepts. The algorithm involves two parts: (i) cluster and centroid the primitives along each bearing strobe, and (ii) associate the range clusters along adjacent bearing angles, then compute a refined range-bearing centroid. The novelty of the approach involves the use of a recursive least squares algorithm with a gating process that is incorporated into the association/clustering procedure.

4.1.1. Perform range clustering and compute partial centroids

The first part of the clustering algorithm involves finding adjacent range cells that have detections. Let $R(n)$ be the range value of the nth range cell. For bearing angle $B(k)$, suppose that we have multiple range cells with detections and the power value for the nth range cell is $P(n,k)$. Denote $\mathcal{I}_k$ as the collection of indices for which adjacent range cells hold detection (for bearing $B(k)$). We group these adjacent cells into *range clusters*, and compute the power-weighted range centroid,

$$\hat{r}(k) = \frac{\sum_{n\in\mathcal{I}_k} P_r(n,k)R(n)}{\sum_{n\in\mathcal{I}_k} P_r(n,k)} \tag{25}$$

If there exists multiple clusters of measurements per bearing angle, $\{\mathcal{I}_k^{(1)},\ldots,\mathcal{I}_k^{(M_k)}\}$, then we obtain a set of centroids for that bearing,

$$\hat{\mathbf{r}}(k) = \{\hat{r}_1(k),\ldots,\hat{r}_M(k)\} \tag{26}$$

For each range estimate $\hat{r}(k)$ we compute an associated partial weight of power values,

$$\hat{w}(k) = \sum_{n\in\mathcal{I}_k} P(n,k) \tag{27}$$

If multiple clusters exist, we compute multiple cluster weights,

$$\hat{\mathbf{w}}(k) = \{\hat{w}_1(k),\ldots,\hat{w}_M(k)\} \tag{28}$$

4.1.2. Perform bearing clustering and compute centroid

Part 2 of the algorithm involves a gating process to associate the range clusters across multiple bearing angles. The range centroid of the target is recursively computed, as the clusters are associated. Let $\hat{R}(k)$ be the centroid estimate of the range using measurements up to bearing k. We identify the best potential range cluster to be the one that is the *nearest neighbor* to the current estimate,

$$\hat{r}^\star(k+1) = \arg\min_j \left|\hat{R}(k) - \hat{r}_j(k+1)\right|, \quad \hat{r}_j(k+1)\in\hat{\mathbf{r}}(k+1) \tag{29}$$

Assign $\hat{w}^\star(k+1)$ to be the corresponding weight. Determine if the next measurement is within the *gate* defined by

$$\left|\hat{R}(k) - \hat{r}^\star(k+1)\right| < \sigma_R \tag{30}$$

where σ_R is a pre-defined gate size. If the closest range value validates (i.e., is within the gate), then we update the estimate of the range position using a Recursive Least Squares processing[14] approach,

$$\begin{aligned}
\hat{R}(k+1) &= \hat{R}(k) + G(k+1)\left(\hat{r}(k+1)^\star - \hat{R}(k)\right) &(31)\\
G(k+1) &= \Sigma(k+1)\cdot\hat{w}(k+1) &(32)\\
\Sigma^{-1}(k+1) &= \Sigma^{-1}(k) + \hat{w}(k+1) &(33)
\end{aligned}$$

The initial conditions for the recursion are $\Sigma_{k_1}^{-1} = \hat{w}_{k_1}$, and $\hat{R}_{k_1} = \hat{r}_{k_1}$, where k_1 is the index to first angle where the target is detected.

If this processing is conducted for a radar that is employing range resolve processing, then the gating and association process must be done for each ambiguous range $\hat{r}_j(k) = \hat{r}(k) + j\cdot R_u$, for $j\in\{0,1,2,\ldots\}$.

4.1.3. State transition logic for target detection

Detection of the target is declared only when a specified number of primitives is found over adjacent angles. To allow for possible missed detections over the sequence of bearing angles, an M-out-of-N logic is employed. A *state machine* is implemented that keeps track of the detection criteria. If we have the condition of

$$\left|\hat{R}(k) - \hat{r}_j(k+1)\right| < \sigma_R, \quad \text{for some } j, \tag{34}$$

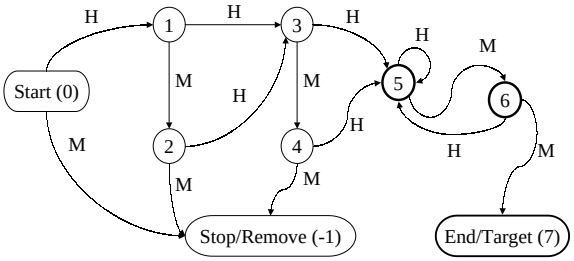

Figure 2. State transition diagram to implement 3-out-of-5 target detection logic.

then we declare a "hit" in the state transition diagram, otherwise a "miss" is declared. The update of the range centroid estimate is done recursively within the state transition model,

$$\hat{R}(k+1) = \begin{cases} \hat{R}(k) + G(k+1)\left(\hat{r}^{\star}(k+1) - \hat{R}(k)\right), & \text{Hit}, \\ \hat{R}(k), & \text{Miss}, \end{cases} \tag{35}$$

Similarly, we compute the bearing angle centroid estimate using the same recursive weighted least squares estimation technique,

$$\hat{B}(k+1) = \begin{cases} \hat{B}(k) + G(k+1)\left(\hat{B}^{\star}(k+1) - \hat{B}(k)\right), & \text{Hit}, \\ \hat{B}(k), & \text{Miss}, \end{cases} \tag{36}$$

The values used for M and N depend on the beamwidth and the scan period of the specific radar. Typically, $N \equiv N_{CPI}$. The value of M is selected based on the unambiguous range requirement in (5).

Two common state machines are used: 2-out-of-3 logic and 3-out-of-5 logic. Figure 2 shows the diagram for the case of 3-out-of-5 logic. The letter "H" represents a hit, while "M" represent a miss. This diagram has a total of seven states. To achieve a target detection, state five must be achieved. Target termination (state seven) requires two misses in a row. Note that once state five is reached, the state machine will stay in state five as long as detections are received. Hence, objects greater than $5\Delta B$ will be maintained as one object.

4.2. Centroid processing with range, bearing, and Doppler

Some surveillance radars are able to make range, bearing, and Doppler (radial velocity) measurements of the target. Computation of the centroid becomes a three-dimensional problem for these sensors, and the algorithm shown above must be modified to include the third dimension (i.e., the Doppler measurement). At bearing angle $B(k)$, suppose that there is one or more measurements in the Doppler bank output of the nth range cell. Each measurement has a separate Doppler frequency and power value, which we denote as $\{f(n,k,\ell), P_r(n,k,\ell)\}$. Here, $\ell \in \{1,\ldots,N_T\}$, where ℓ is the index to the Doppler filter number and N_T is the total number of targets detected in the nth range cell at bearing angle $B(k)$.

The measurements in the nth range cell must be grouped (clustered) with those in adjacent range cells. The first step in the extended algorithm is to simultaneously cluster measurements in Doppler and range along each bearing angle. Let $\mathcal{I}_k$ denote the set of adjacent range cell indices for which there are measurements at bearing angle $B(k)$. Within the set, we find the indices (range and Doppler) corresponding to the largest peak,

$$(n^{\star}, \ell^{\star}) \leftarrow \arg\max_{n,\ell} P(n,k,\ell), \quad n \in \mathcal{I}_k, \ell \in \{1,\ldots,N_T\} \tag{37}$$

Let $f^\star = f(n^\star, k, \ell^\star)$, be the measured Doppler frequency corresponding to the peak value within the cluster of adjacent range bins. Measurements in the adjacent range bins are clustered provided each cell has a measurement with a Doppler value within a Doppler gate centered on $f^\star$. That is, provided that there exists an index ℓ such that

$$|f(n,k,\ell) - f^\star| < \sigma_F, \quad \forall n \in \mathcal{I}_k \tag{38}$$

then the adjacent range bins can be clustered. If more than one measurement exists within the Doppler gate, then we select the closest one,

$$\ell_n \leftarrow \arg\min_\ell |f(n,k,\ell) - f^\star| \tag{39}$$

where ℓ_n represents the selected Doppler bin index for the nth range bin.

Now, the set $\mathcal{L}_k = \{\ell_n : n \in \mathcal{I}_k\}$ denotes the Doppler bin indices in the range cluster used in the clustering operation. If no measurement exists for a given range bin such that (38) and (39) hold, then there is a break in the cluster (i.e., measurements in bins $n-1$ and n form separate clusters). Once a validated set of range bins is identified, we compute the weighted estimate of the range and the Doppler frequency,

$$\hat{r}(k) = \frac{\sum_{n\in\mathcal{I}_k, \ell\in\mathcal{L}_k} R(n) P_r(n,k,\ell)}{\sum_{n\in\mathcal{I}_k, \ell\in\mathcal{L}_k} P_r(n,k,\ell)} \tag{40}$$

$$\hat{f}(k) = \frac{\sum_{n\in\mathcal{I}_k, \ell\in\mathcal{L}_k} f(n,k,\ell) P_r(n,k,\ell)}{\sum_{n\in\mathcal{I}_k, \ell\in\mathcal{L}_k} P_r(n,k,\ell)} \tag{41}$$

If multiple Doppler filter measurements are present within one range bin, clustering can be repeated to find multiple targets. Once the set $\mathcal{L}_k$ is identified within a range bin cluster, those primitives can be pulled from consideration and the process repeated starting with (37). A new set of measurements $\mathcal{L}_k^{(2)}$ can be obtained and the centroid computed for these primitives.

After centroids have been computed for each bearing angle, then the measurement can be clustered over multiple bearing angles as is done above. The only caveat is that the association process has to be done in both the range and Doppler domains. Within the recursive weighted least squares estimation process, let $\hat{R}(k)$ be the present range estimate and $\hat{F}(k)$ be the Doppler frequency estimate. The candidate measurement at the next bearing angle for inclusion in the cluster is selected as the nearest neighbor,

$$\left(\hat{r}^\star(k+1), \hat{f}^\star(k+1)\right) \leftarrow \arg\min_j \left(\frac{\left|\hat{R}(k) - \hat{r}_j(k+1)\right|^2}{\sigma_R^2} + \frac{\left|\hat{F}(k) - \hat{f}_j(k+1)\right|^2}{\sigma_F^2} \right) \tag{42}$$

This measurement is included provided that $\left|\hat{R}(k) - \hat{r}_j(k+1)\right| < \sigma_R$ and $\left|\hat{F}(k) - \hat{f}_j(k+1)\right| < \sigma_F$, otherwise a "miss" occurs and no measurement is included at bearing angle $B(k)$.

4.3. Merged measurement handling within the centroid processing algorithm

In military applications, it is possible that there will be multiple closely spaced air targets (e.g., a formation of fighter planes). When the spacing between the planes is equal to or less than the range/bearing resolution of the surveillance radar, then the centroid processing will merge the primitives from all targets into one single object. The reported measurement will have the position that is the centroid of the targets. In some instances, the merged measurements might be considered a good thing: only one report is needed to cue a tracking radar. But if a complete air picture is desired, then the merging of targets into a single object is not desired.

There are different ways to handle the merged measurement problem within the centroid processing algorithm, and we will only sketch the ideas here. First, one will want to *detect* the presence of merged measurements. This can be done by evaluating the range and bearing extent of the reported object. If small (single range-bearing cell size) targets are expected, and the report extends beyond the $2 \times N_{CPI}$ range-bearing cells, then multiple targets can be expected. Also, using the beamshape fitting concept of Cole[1] et al. would allow for multiple-target detection.

Once the presence of multiple targets has been detected, then a *parsing* algorithm is required to break the primitives into multiple object sets. To accomplish this, one typically looks for the largest change in the primitive

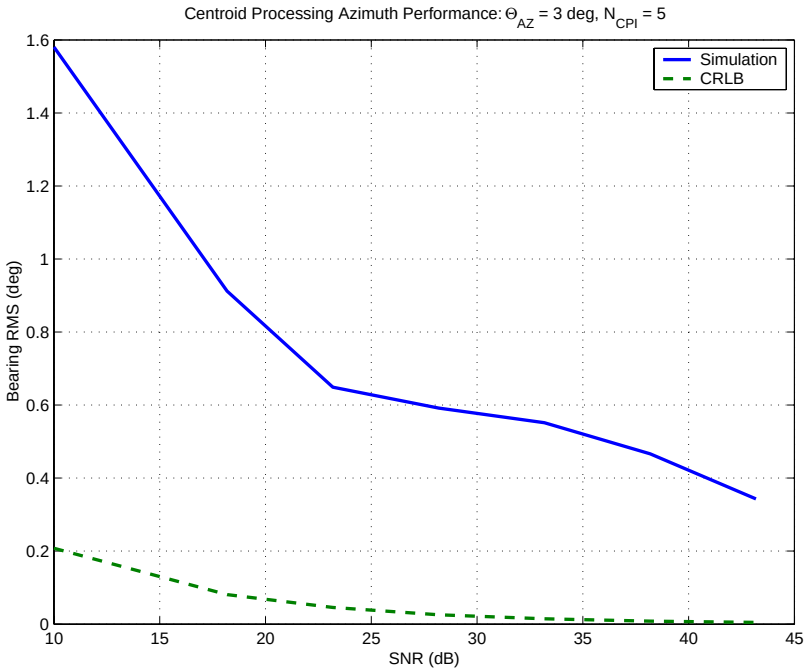

Figure 3. Centroid processing bearing estimation simulation results.

measurements between adjacent cells. For example, if we define $\Delta\hat{r}(k) = \hat{r}(k+1) - \hat{r}(k)$, then by identifying the index k within an object cluster that produces the largest $\Delta\hat{r}(k)$ could be used as the point to separate the primitives into two sets. Similarly, this could be done in the Doppler dimension.

Another potential way to improve merged measurement handling is to include feedback from the target tracker when the primitives are separated into object clusters. Therefore, if two targets are initially separated and then come together, the knowledge of the multiple objects present in the track database could be used by the centroiding algorithm to parse the primitive measurements.

5. SIMULATION RESULTS

The range-bearing centroid processing algorithm described in Section 4 was implemented in a tracking simulation. The radar was modeled to have a 3.0° beamwidth and switched among $N_{CPI} = 5$ separate PRIs as the beam scanned a target. Figure 3 shows the azimuth estimation accuracy achieved in the simulation. For high SNR conditions, the accuracy approximates 0.5°. Hence, the azimuth estimation is improved by a factor of $3.0^\circ/0.5^\circ = 6$. Also plotted is the CRLB from (7) where N_{CPI} was used instead of N_{AZ}. As shown, the performance achieved in the simulation is many times worse than the bound. As discussed in Section 2.4, it is questionable whether the bound is valid for the coherent radar model, and the simulation results suggest as much.

6. CONCLUSIONS

In surveillance radars, the problem of associating and clustering primitive measurements into object reports with refined range-bearing estimates is accomplished by a centroid processing algorithm. In this paper, we reviewed a number of techniques used for centroid processing: moving window estimator, two-pole filter and maximum output estimator, the maximum likelihood (Bernstein) estimator, and a beam shape estimator. We also presented a new center of mass algorithm that utilizes a weighted recursive least squares algorithm. Simulation results were shown to characterize the azimuth estimation accuracy versus SNR. Potential techniques for handling merged measurement conditions within the centroid processing algorithm were discussed.

REFERENCES

1. E. L. Cole, M. J. Hodges, R. G. Oliver, and A. C. Sullivan, "Novel accuracy and resolution algorithms for the third generation MTD," *Proceedings of the 1986 National Radar Conference* , pp. 41–47, 1986.
2. M. I. Skolnik, *Radar Handbook*, McGraw-Hill, New York, 2nd ed., 1990.
3. G. V. Morris, "Selection of the medium PRFs," in *Airborne Pulse Doppler Radar*, G. V. Morris, ed., ch. 11, Artech House, 1988.
4. W. D. Blair and B. M. Keel, "Radar systems modeling for tracking," in *Multitarget-Multisensor Tracking: Applications and Advances*, Y. Bar-Shalom and W. D. Blair, eds., ch. 7, Artech House, 2000.
5. P. Swerling, "Maximum angular accuracy of a pulsed search radar," *Proceedings of the IRE* , pp. 1146–1155, September 1956.
6. D. K. Barton, *Radar System Analysis*, Artech House, Dedham, MA, 1976.
7. M. I. Skolnik, *Introduction to Radar Systems*, McGraw-Hill, New York, 1980.
8. C. M. Walker, J. Atkin, and H. Bickel, "Comparative evaluation of several azimuth estimating procedures using digital processing and search radar simulation," *IRE Transactions on Aeronautical and Navigational Electronics* , pp. 114–121, June 1958.
9. G. Galati and F. A. Struder, "Angular accuracy of the binary moving window radar detector," *IEEE Transactions on Aerospace and Electronic Systems* **18**, pp. 416–422, July 1982.
10. B. H. Cantrell and G. V. Trunk, "Angular accuracy of a scanning radar employing a two-pole filter," *IEEE Transactions on Aerospace and Electronic Systems* **9**, pp. 649–653, September 1973.
11. D. C. Cooper and J. W. R. Griffiths, "Video integration in radar and sonar systems," *Journal of British IRE* **21**, pp. 421–433, May 1961.
12. R. Bernstein, "An analysis of angular accuracy in search radar," *IRE National Convention Record* **3**(5), pp. 61–78, 1955.
13. G. Galati and F. A. Struder, "Maximum likelihood azimuth estimation applied to SSR/IFF systems," *IEEE Transactions on Aerospace and Electronic Systems* **26**, pp. 27–43, January 1990.
14. J. M. Mendel, *Lessons in Digital Estimation Theory*, Prentice Hall, Englewood Cliffs, N.J., 1987.